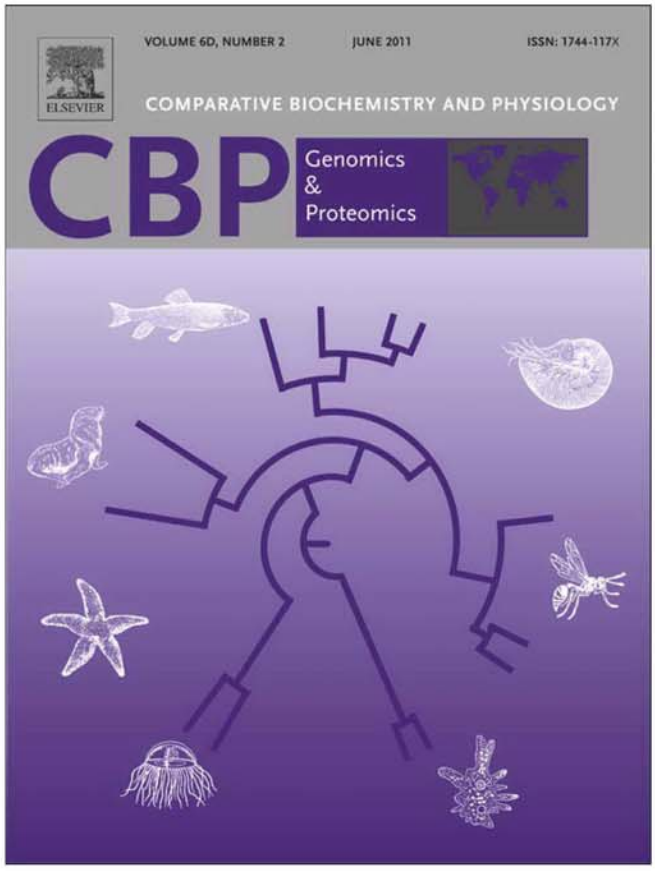

Comparative Biochemistry and Physiology, Part D 6 (2011) 213–223

Contents lists available at ScienceDirect

Comparative Biochemistry and Physiology, Part D

journal homepage: www.elsevier.com/locate/cbpd

Differentiating size-dependent responses of juvenile pink salmon (*Oncorhynchus gorbuscha*) to sea lice (*Lepeophtheirus salmonis*) infections

Ben J.G. Sutherland [a], Stuart G. Jantzen [a], Dan S. Sanderson [a], Ben F. Koop [a,*], Simon R.M. Jones [b]

[a] Centre for Biomedical Research, University of Victoria, Victoria, British Columbia, Canada V8W 3N5
[b] Pacific Biological Station, 3190 Hammond Bay Road, Nanaimo, British Columbia, Canada V9T 6N7

ARTICLE INFO

Article history:
Received 25 February 2011
Received in revised form 8 April 2011
Accepted 11 April 2011
Available online 15 April 2011

Keywords:
Cell proliferation
Conservation
Development
Immune system
Inflammation
Pink salmon
Sea lice
Transcriptomics

ABSTRACT

Salmon infected with an ectoparasitic marine copepod, the salmon louse *Lepeophtheirus salmonis*, incur a wide variety of consequences depending upon host sensitivity. Juvenile pink salmon (*Oncorhynchus gorbuscha*) migrate from natal freshwater systems to the ocean at a young age relative to other Pacific salmon, and require rapid development of appropriate defenses against marine pathogens. We analyzed the early transcriptomic responses of naïve juvenile pink salmon of sizes 0.3 g (no scales), 0.7 g (mid-scale development) and 2.4 g (scales fully developed) six days after a low-level laboratory exposure to *L. salmonis* copepodids. All infected size groups exhibited unique transcriptional profiles. Inflammation and inhibition of cell proliferation was identified in the smallest size class (0.3 g), while increased glucose absorption and retention was identified in the middle size class (0.7 g). Tissue-remodeling genes were also up-regulated in both the 0.3 g and 0.7 g size groups. Profiles of the 2.4 g size class indicated cell-mediated immunity and possibly parasite-induced growth augmentation. Understanding a size-based threshold of resistance to *L. salmonis* is important for fisheries management. This work characterizes molecular responses reflecting the gradual development of innate immunity to *L. salmonis* between the susceptible (0.3 g) and refractory (2.4 g) pink salmon size classes.

1. Introduction

The salmon louse *Lepeophtheirus salmonis* (Copepoda: Caligidae) is an ectoparasitic marine copepod that infects wild and farmed salmonids in the Northern Hemisphere (Nagasawa et al., 1993; Jones, 2009). The life cycle consists of two free-swimming larval stages (nauplius I, II) an infectious copepodid stage and seven parasitic stages (chalimus I–IV, pre-adult I–II and adult; Johnson and Albright, 1991). Parasitic stages predominantly feed upon host epidermis and mucus, and occasionally blood (Bron et al., 1993; Johnson and Albright, 1991). Chalimus stages are relatively small and tethered to the host by a frontal filament, whereas later pre-adult and adult stages are larger, motile, and more damaging to the host (Grimnes and Jakobsen, 1996; Mackinnon, 1993). *L. salmonis* infections have serious economic and ecological implications among valuable salmon populations (Costello, 2006).

In the susceptible Atlantic salmon (*Salmo salar*) the effects of *L. salmonis* infection include changes in plasma cortisol, glucose and ion concentration (Bowers et al., 2000; Finstad et al., 2000; Grimnes and Jakobsen, 1996; Wagner et al., 2003), changes in mucus lysozyme and alkaline phosphatase presence and activity (Easy and Ross, 2009; Fast et al., 2002), skin damage, reduced growth and food conversion, behavioral changes, and stress-induced mortality (reviewed in Costello, 2006; Wagner et al., 2008). Stress responses can be attributed to both feeding mechanisms and immune-modulatory salivary secretions of the louse (Fast et al., 2005; Firth et al., 2000). Molecular evidence of tissue remodeling without accompanying wound healing indicates the infections in Atlantic salmon are chronic (Skugor et al., 2008).

Variation in susceptibility to *L. salmonis* occurs among salmon species (Johnson and Albright, 1991; Nagasawa et al., 1993; Fast et al., 2002; Jones et al., 2007). Therefore it is important to understand the interactions of *L. salmonis* with a variety of host species (Costello, 2006; Wagner et al., 2008). In laboratory exposures, coho salmon (*Oncorhynchus kisutch*) exhibit the greatest resistance to louse infection (Fast et al., 2002), a response attributed to early inflammation (Johnson and Albright, 1992).

A size-dependent sensitivity to *L. salmonis* was identified in juvenile pink salmon (Jones et al., 2008). In this laboratory exposure of pink salmon, the average intensity of infection at 6 days post exposure (dpe) was similar, with 4.9, 3.0, and 2.8 lice per fish (lpf) among 0.3 g, 0.7 g, and 2.4 g size classes, respectively. However, by 37 dpe the infection prevalence was much higher in the 0.3 g and 0.7 g groups (36.4% and 35%, respectively) than in the 2.4 g size class (5%). Furthermore, significant mortality occurred solely in the 0.3 g

* Corresponding author at: Centre for Biomedical Research, University of Victoria, P. O. Box 3020 STN CSC, Victoria, British Columbia, Canada V8W 3N5. Fax: +1 250 472 4075.
E-mail address: bkoop@uvic.ca (B.F. Koop).

1744-117X/$ – see front matter © 2011 Elsevier Inc. All rights reserved.
doi:10.1016/j.cbd.2011.04.001

size class and mostly occurred after 13 dpe (0.3 g mortality ~37%; 0.7 g mortality ~5%; 2.4 g no mortality). The pattern of louse development was similar on all size groups, with mainly copepodids present at 6 dpe (one chalimus I was identified on a 2.4 g fish), and chalimus I and II present at 12 dpe. In this exposure, 80.9% of lice on dead fish were chalimus IV stage or earlier. The absence of significant mortality in the 0.7 g and 2.4 g pink salmon indicates an onset of protection between the 0.3 g and 0.7 g size classes (Jones et al., 2008). To further understand the mechanisms behind these variable responses, we have profiled transcriptomes of the three size classes of juvenile pink salmon from the aforementioned exposure trials (Jones et al., 2008). Using both a 32K cDNA microarray and qRT-PCR, we investigated the responses at 6 dpe, before significant mortality occurs, to investigate the primary host responses to early stages of lice.

2. Materials and methods

2.1. Animals

A complete description of the source and maintenance of animals was previously reported (Jones et al., 2008). Briefly, juvenile pink salmon were derived from a naturally spawned, gravel-reared population and collected with in-river rotary screw traps from the Glendale River on the central coast of British Columbia (BC) in April 2007. Fry were transported to and maintained at Pacific Biological Station (Nanaimo, BC, Canada) in 400 L stock tanks with a mixture of flow-through dechlorinated fresh water and sand-filtered sea water. Salmon were fed a crumble (0 and 1) ration (Ewos, Canada Ltd., Surrey, BC, Canada) at an average daily rate of 1.2% body weight. Salmon were acclimatized to seawater for one week prior to experimental challenges.

Gravid lice were obtained from Atlantic salmon from commercial net pens near Vancouver Island. Egg strings were dissected, hatched at 32.5‰ salinity and 8.9 °C, and incubated for one week at which time an inoculum containing a known number of copepodids was created by pooling incubation beakers.

2.2. Louse exposure and tissue extraction

A complete description of exposure methodology was previously reported (Jones et al., 2008). Briefly, three separate trials with different size groups of salmon were conducted. The mean weights (±SE) of salmon at the beginning of each trial were 0.25 ± 0.01 g, 0.69 ± 0.02 g, and 2.37 ± 0.04 g. In each trial, fish were exposed at a rate of 100 copepodids per fish. The exposure was performed by halting water flow, reducing volume to 3 or 4 L with supplemental aeration, and sedating fish with 0.07 mg/L metomidate·HCl. The copepodid inoculum was added, tanks were then kept dark for 2 h, and then water flow was resumed. Fish were then maintained at 12 h light then 12 h dark photoperiods. For all trials, mean temperature and salinity were 8.9 °C (range, 7.7–9.6 °C) and 32.5‰ (range, 28–34‰), respectively. Control fish with the same history were treated the same as the experimental fish, but without the addition of copepodids. All treatments and control groups were maintained and challenged in duplicate tanks.

At 6 dpe fish were sedated and 10 uninfected and 10 infected fish were killed in an overdose of MS-222 (Syndel). Each fish was rapidly processed (mass and length measured, louse number and molt stage recorded, flash frozen in liquid nitrogen and stored at −80 °C) to preserve RNA quality (Jones et al., 2008).

2.3. RNA preparation

Tissue cross-sections of approximately 2 mm thick were obtained from frozen fish by making parallel bisections anterior to the dorsal fin. The still-frozen tissue was placed directly into TRIZOL® and homogenized with a *TissueLyser II* (Qiagen, Valencia, CA, USA). Total RNA was extracted as per manufacturer's instructions (Invitrogen), and purified through RNeasy spin columns, as per manufacturer's instructions (Qiagen). Total RNA was quality-checked with agarose gel electrophoresis, quantified by spectrophotometry (NanoDrop Technologies, Wilmington, DE, USA), and stored at −80 °C.

2.4. Synthesis of experimental channel (cDNA) and reference channel (aRNA) samples

Six individuals from each condition were randomly selected for cDNA synthesis (three per tank, 12 per size group, 36 total). Using a Superscript™ Indirect cDNA Labeling System (Invitrogen), cDNA was synthesized as previously reported (von Schalburg et al., 2005). In brief, 10 μg total RNA was primed with oligo$(dT)_{20}$ primers and reverse transcribed to incorporate amino-allyl-modified nucleotides. Modified cDNA was labeled with Mono-Reactive Cy5™ dye in a 2 h reaction in coupling buffer (Amersham Biosciences), purified using S.N.A.P. columns (Invitrogen), quantified through spectrophotometry (NanoDrop Technologies), and kept dark and cool until hybridization.

An aRNA reference pool was synthesized from total RNA obtained from juvenile pink salmon representing a variety of size and infection conditions. Reference aRNA was synthesized using the Amino-Allyl MessageAmp™ aRNA kit (Applied Biosystems, Austin, TX, USA) as per manufacturer's instructions. In brief, 2 μg total RNA was reverse-transcribed with T7 oligo$(dT)_{20}$ primers and reverse transcriptase. Second strand cDNA was synthesized using DNA polymerase, then purified using cDNA Filter Cartridges. aRNA was then synthesized through in vitro T7 transcription with amino-allyl modified UTPs, purified with aRNA Filter Cartridges, and quantified using spectrophotometry (NanoDrop Technologies). Equimolar amounts of aRNA from each of the eight samples were pooled, aliquoted, and stored at −80 °C until labeling. Labeling of the aRNA was the same as described above for the cDNA, except with Mono-Reactive Cy3™ dye. Labeled cDNA (250 ng) and aRNA (500 ng) were combined and brought up to 23 μl with RNase-free water (Invitrogen) and kept dark at 4 °C.

2.5. Microarray hybridization, scanning, and spot quantification

Samples were hybridized to a single batch of cGRASP salmonid 32K cDNA microarrays (http://web.uvic.ca/grasp/microarray/array.html) using a Tecan Pro HS 4800™ Hybridization Station (Tecan Group Ltd., Männedorf, Switzerland). The cGRASP microarray has been fully described (Koop et al., 2008). The array was designed to consist of 27,917 Atlantic salmon and 4065 rainbow trout cDNA elements, and can be used for hybridizations of all 68 members of Salmonidae, including pink salmon (Koop et al., 2008).

The microarray hybridization protocol was adapted from previous work (Koop et al., 2008). All slides were pre-washed with 0.1X SSC, 0.2% SDS three times for 30 s at 23 °C, 0.2X SSC two times for 60 s at 23 °C and once with 5X SSC, 0.01% SDS, 0.2% BSA for 60 s at 49 °C. The final pre-wash solution was incubated for 1 h at medium agitation to block non-specific binding of the array. Slides were then washed twice with 2X SSC, 0.014% SDS for 60 s at 49 °C. To each sample, 2 μl LNA dT blocker (Genisphere LLC., Hatfield, PA, USA) and 100 μl hybridization buffer at 65 °C (Applied Biosystems,) were added and heated to 80 °C for 10 min, then kept at 65 °C until sample loading. Hybridization occurred over 16 h with periodical hourly temperature oscillations of 49 °C and 53 °C. Following incubation, slides were washed with 2X SSC, 0.014% SDS for 60 s at 49 °C, incubated for 3 min, washed at 49 °C for 60 s, at 39 °C for 20 s, and at 30 °C for 20 s. Slides were finally washed with 1X SSC for 60 s at 23 °C and with 0.2X SSC for 30 s at 23 °C, dried with 255 kPa nitrogen gas and kept dark in a low-ozone environment (ozone ≤ 0.005 ppm) and scanned as soon as possible with a ScanArray® Express (PerkinElmer, Inc., Waltham, MA; 5 μm

resolution; PMTs: Cy5:74, Cy3:76; ozone ≤ 0.016 ppm). Fluorescence intensity data and quality measures were extracted using ImaGene® 8.0 (BioDiscovery, El Segundo, CA, USA).

Array element identification and annotation was assigned by the cGRASP consortium (http://web.uvic.ca/cbr/grasp) and has previously been reported (Koop et al., 2008; von Schalburg et al., 2005). The annotation file can be found at http://web.uvic.ca/grasp/microarray/array.html.

2.6. Microarray normalization, filtering, and analysis

Data normalization and analysis was performed with GeneSpring™ GX11 (Agilent). Raw signal was transformed to a threshold of 1.0. Arrays were normalized using a per-slide, per-block intensity-dependent Lowess normalization and a per-sample, per-gene baseline to median normalization. Data files were deposited in NCBI's Gene Expression Omnibus under the accession GSE27528 (http://www.ncbi.nlm.nih.gov/geo/). Due to technical limitations for comparing expression differences across size groups, as discussed in Section 3.1, direct comparisons were only made within a size class. For each size class, normalized spot values, or entities, were filtered to only retain those in which at least 65% of the samples in at least one of the two conditions (exposed or control) had raw signal greater than or equal to 500. Entities were then filtered using volcano plot (Mann–Whitney $p \leq 0.05$, no multiple test correction, and fold change (FC) ≥ 2).

Functions over-represented in each size group's differential gene list were investigated using Gene Ontology and pathway annotation. Differentially expressed entity lists (FC ≥ 2, $p \leq 0.05$) were used as an input into the GX11 GO browser (Agilent), and enriched categories were retained ($p \leq 0.05$, no multiple test correction). GO Trimming was performed on the significantly enriched GO lists in order to reduce redundancy in displayed tables. This algorithm reduces redundancy by removing overlapping terms from the enriched GO category list through the removal of parent terms if they contain less than 40% unique entity content when compared to the child term. This procedure is fully described elsewhere (Jantzen et al., in review), and does not change enrichment values of terms, but rather just systematically selects a subset of terms to be discussed.

For each size group, differentially expressed genes (FC ≥ 2, $p \leq 0.05$) with Gene ID annotation were used for Find Significant Pathways analysis (Agilent) and enriched pathways ($p \leq 0.05$) were retained.

2.7. Quantitative real-time polymerase chain reaction (qRT-PCR)

The same individual RNA samples included in the microarray analysis were used for qRT-PCR. Briefly, cDNA was synthesized using the SuperScript® III First-Strand Synthesis System for RT-PCR (Invitrogen), as per manufacturer's instructions, and as described in Section 2.2 for first strand modified cDNA but with unmodified dNTPs. Genes of interest (GOI) were selected from microarray results due to high fold change, involvement in enriched GO categories from either the present investigation or a previous microarray investigation (data unpublished), or to compare to trends identified in the response of Atlantic salmon to sea lice infection (Skugor et al., 2008). Primers used are shown in Table 2, and were designed using Primer3 (Rozen and Skaletsky, 2000) and AlleleID®7.0 (PREMIER Biosoft International, Palo Alto, CA, USA) based on conserved sequences from available data for salmonid species, including *S. salar*, *Oncorhynchus mykiss*, *Oncorhynchus nerka* and in some cases *Danio rerio*. The original sequence used as the search query was the contiguous sequence (contig) of the cDNA element of interest on the microarray. All related sequences were obtained from NCBI or the cGRASP database (cGRASP; http://lucy.ceh.uvic.ca/contigs/cbr_contig_viewer.py).

Equimolar amounts of all samples from all conditions investigated ($n = 36$) were pooled, diluted two-fold, and then used as a starting point for a five point, five-fold standard dilution series to be used as a standard curve for testing primer amplification efficiencies (Table 2). This series was also run in duplicate as a positive control during each GOI plate run. Experimental samples, −RT and no template control (NTC) were also run in duplicate on a single plate for each GOI. qRT-PCR was performed in 20 µl reactions using SYBR GreenER™ qPCR SuperMix Universal master mix as per manufacturer's instructions (Invitrogen) in an Mx3000P™ thermal cycler (Agilent). The following thermal regime was used for all samples: Segment 1, 95 °C for 120 s, 1 cycle; Segment 2, 95 °C for 15 s, 55 °C for 30 s (fluorescence read at end), 72 °C for 20 s, 40 cycles; and Segment 3, 95 °C for 60 s, 55 °C for 30 s, and then ramp up to 95 °C for 30 s (fluorescence read each 0.5 °C increment).

Quality control of duplicate wells permitted a standard deviation of less than one Ct. In order to confirm amplicon identity and singularity, melt curve analysis and amplicon sequencing were performed. All GOIs reported displayed a single product. Each amplicon was purified post-qRT-PCR with SureClean™, as per manufacturers' instructions (Bioline), and sequenced bi-directionally by BigDye® Terminator sequencing as per manufacturer's instructions (Applied Biosystems) in 5 µl reactions with 1 µl of 3.2 µM gene-specific forward or reverse primer, BigDye®, and 2.5 ng of template cDNA. The sequencing reaction thermal regime was as follows: Segment 1, 95 °C for 60 s, 1 cycle; Segment 2, 95 °C for 30 s, 50 °C for 15 s, 60 °C for 90 s, 35 cycles; Segment 3, 60 °C for 5 min, 1 cycle. PCR products were then ethanol precipitated and run on a 3730 DNA Analyzer (Applied Biosystems), as per manufacturer's instructions, with an injection time of 15 s. Trace files were interpreted using a short-read analysis algorithm (Applied Biosystems). All sequences corresponded to the expected amplicon.

A representative sample from each group was included as a negative reverse transcriptase (−RT) control. −RT samples were tested with primer pairs for sestrin-1 and ubiquitin and amplified by PCR with GoTaq® (Promega, Madison, WI, USA) with the thermal regime used for qRT-PCR. PCR products were viewed on a 1% agarose gel, and the samples with the most product after 40 cycles were included in each qRT-PCR run as a −RT control. The difference between the −RT and the +RT sample was greater than 6 Ct (Qiagen), and the NTC remained clean.

Normalizer gene candidates were selected based on static expression in microarray results: eukaryotic translation initiation factor 4H (*eif4h*), actin cytoplasmic 1 (*actb*), ubiquitin and plastin-1. Transcript expression stability was investigated using geNORM algorithms (Vandesompele et al., 2002). After removal of the least stable normalizer candidates, *eif4h* and *actb* had an *M* value of 0.4279 and CV of 14.92%, values within necessary criteria for stable normalizer genes (Vandesompele et al., 2002; Pérez et al., 2008). Normalization of experimental samples was performed with the geometric mean of these two normalizers (Vandesompele et al., 2002). Relative quantities were determined using primer-specific amplification efficiencies (Table 2) in REST© v.2.0.13 (Qiagen), and statistical significance was determined by a Pair Wise Fixed Reallocation Randomization Test© (Pfaffl et al., 2002).

Table 1
Intensity of infection (average lice/fish (range)) at 6 dpe for 0.3 g, 0.7 g, and 2.4 g pink salmon (data from Jones et al., 2008), and total entities differentially expressed (FC>2; $p \leq 0.05$) for each size group.

Size (g)	Avg (range) lice per fish at 6 dpe	Total entities up-regulated (FC>2; $p \leq 0.05$)	Total entities down-regulated (FC>2; $p \leq 0.05$)
0.3	4.9 (1–8)	281	308
0.7	3.0 (1–5)	1282	1843
2.4	2.8 (1–8)	296	174

3. Results

3.1. Microarray size-dependent expression profiles

The use of the cGRASP 32K salmonid cDNA array enabled the investigation of global gene expression changes of the early response

Table 2
Primer sequences used in PCRs. Includes sense and antisense primers, putative product size and efficiency values.

GOI	Sense primer	Antisense primer	Product size	R^2	Effic. (%)
actb	CCTCCTTCCTCGGTATGG	ATGTCCACGTCACACTTC	76	0.99	87.1
eif4h	CACAGTACAAGGAGACATAG	AGGAGAGCACCATCATAC	162	0.99	92.2
pls1	ATAATCAACTGGGTCAAC	TGTCTAACAAGTCTATCAC	112	1.00	99.2
ubiq	TTCTGTTCTGGCAAATGTTC	TTCCTATACTTCATAAGTTCCATTG	147	0.98	96.5
tob1	CCTCAACTTTATTATTTCC	CCTTATATGGCTTATCAG	131	0.95	104.4
cdkn2b	ATCCTTGTCCAATTCCTC	ACTTTCTATTGCCAAATCG	78	0.99	96.0
sesn1	TTCCAGCACTCCGAGAAG	TCAGAGCGTAGAGCAGTTC	79	1.00	102.9
btg1	GCTGTCTACTCTACCTTG	TACAACTTTCGCACAATC	130	0.98	97.2
tfdp1	CTTCAGACAGAGCCTTAC	ACCTTCAGTTCTCCATTG	82	0.98	96.1
sod1	TACCGGGACCGTATTCTTTG	TCTCCATAAGCATGGACGTG	114	1.00	99.7
tgfbr1	AAGGAGTTTGCTTCGTGTCC	ATGGGGTAGATGCCAGTGTC	148	1.00	91.5
fkbp7	ACATTCTACTTCAAGGTG	TTATCAATCCATCTCTATCG	121	0.99	96.0
tia1	ATGGGTAAGGAGGTTAAAG	ATGGAAATGATTGCTTGTG	75	0.99	101.9
ifi30	CTTGGATTGTCATAAATGG	TAACTTCTGTGTCGTTTC	142	0.99	100.3
mmp9	TTTCTCGGGGAGACATATGAAG	TCAGAGTTTCCACCAATCACAG	146	1.00	94.8
mmp13	GCTTCACCACCTTCGACAAT	ATGGAGTTGTCCACCTCAGC	103	1.00	99.3
timp2	TATCGACGCCATCTTCACTG	ATACTCCTTGTTGCCGTTGG	76	1.00	95.4
ttn1	ATGGAAGTTGAAGGCCACAG	TCTCCAGGCACATCCTCTTC	149	1.00	101.4
iqgap1	TAAGGCACATAATGAATAC	GAACAGAACATCTAACAG	100	1.00	102.6
smarce1	ACTACAGGCTGGGAGGGAAT	TTGGAGGCTTTGACTTGGTC	145	1.00	96.8
pdia3	CCAGTGATCCCAACATTG	GGCTCATTTTCTGTCCAG	120	1.00	99.6
prex1	ATCAAGAGGGTCTGCTTC	CTGTTACTGTTACATTCACTG	101	0.97	90.0
rpp21	ACAACCTATTAGCATTACATC	TCGTTCCTGAACTTACTG	147	0.96	95.3
dusp26	TGGTGGCTATTAAAGAAC	TCCGATGTAGAGATTAGG	92	0.98	105.2
sugt1	GCTCCGATAACACTTTCC	TCTCCTTTCCATTCTGATTG	78	0.99	97.4

of three size groups of post-smolt pink salmon (0.3 g, 0.7 g, and 2.4 g) to a low-level lice infection. Due to the large quantity of changed expression (Table 1), further analytical methods were applied to the gene list and these guided the interpretation of gene profiles.

Shared differentially expressed genes were rare among the size groups (Fig. 1). Less than ten entities were common to all size classes in either the up or down-regulated direction, and the greatest similarity was found in the intersect of the 0.3 g and 0.7 g gene lists.

Differentially regulated genes with the highest up- or down-regulated fold change (FC) from each size group are presented in Tables 3a, 3b, 4a, 4b, 5a and 5b. The total differential gene lists can be found in Additional File 1.

3.1.1. 0.3 g salmon

Up-regulated genes with the highest fold change (FC>3; Table 3a) included 20S proteasome subunit alpha type-1, and sterile alpha motif domain-containing protein 9, which is involved in in vitro cell proliferation inhibition (Li et al., 2007).

Several down-regulated genes with the highest fold change (FC>3; Table 3b) included exportin-1 (FC=20.7) and FK506-binding protein 1A, both of which have been identified as up-regulated during cell-cycle progression (Kudo et al., 1997). Additionally, hemicentin-1, a conserved matrix protein with involvement in epidermis development in *Caenorhabditis elegans* (Vogel and Hedgecock, 2001), was down-regulated.

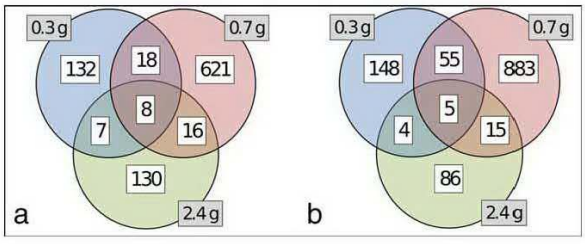

Fig. 1. Differentially expressed genes unique or common among size groups of infected pink salmon. Diagram displays the numbers of differentially expressed transcripts (FC>2; $p \leq 0.05$) shared among size groups in the a) up- or b) down-regulated directions.

3.1.2. 0.7 g salmon

Many genes displayed high fold change expression changes in the 0.7 g list, and those with the highest are displayed in Table 4a (FC>7). Both sodium/glucose co-transporter 1 (*sglt1*) and 2 (*sglt2*) were up-regulated (FC>4.5, $p<0.02$; Additional File 1), and are involved in transporting sugar from the gut lumen (*sglt1*), or re-absorbing from the glomerular filtrate (*sglt2*; Wright and Turk, 2004). Other transcripts up-regulated are involved in cell motility, including talin-1 and intraflagellar transport protein 46 (Burridge et al., 1988; Hynes, 1992; Hou et al., 2007).

Genes down-regulated with high fold change are displayed in Table 4b (FC>4). Isotocin, the oxytocin homologue in bony fishes was down-regulated (FC=5.9), as was titin, a major component of vertebrate striated muscle (Labeit and Kolmerer, 1995). Myosin-9 (FC=5.5) and tubulin alpha-1B chain (FC=5.1, $p<0.02$; Additional File 1) were down-regulated, and are involved in cell structure.

3.1.3. 2.4 g salmon

Genes with the highest up-regulated fold change in the 2.4 g size class are displayed in Table 5a (FC>3). The transcript with the highest fold change was acidic mammalian chitinase (AMCase) precursor, involved in both chitin degradation and immune responses (FC=8.6). Stress suppression-related transcripts protein phosphatase 1L,

Table 3a
Up-regulated genes in the 0.3 g infected pink salmon with highest fold change (Mann–Whitney unpaired $p \leq 0.05$). Genes discussed in the text are in bold font.

Gene description	Up-reg FC	p-value	GenBank
SWI/SNF-related matrix-associated actin-dependent regulator of chromatin subfamily E member 1	5.44	0.004	CB507773
SAPS domain family member 3	4.72	0.010	DY732411
VAR1 Mitochondrial ribosomal protein	4.67	0.016	CA063979
Vang-like protein 1	4.36	0.010	DW583738
Proteasome subunit alpha type-1	4.23	0.025	CA043404
Sterile alpha motif domain-containing protein 9	4.22	0.025	EG758275
LYR motif-containing protein 1	3.95	0.010	EG920165
Alpha-protein kinase 1	3.89	0.025	CB518092
Beta-2-glycoprotein 1 precursor	3.80	0.037	CA037450
Palatin-like phospholipase domain containing protein-4	3.72	0.010	CA045263

Table 3b
Down-regulated genes in the 0.3 g infected pink salmon with highest fold change (Mann–Whitney unpaired $p \leq 0.05$). Genes discussed in the text are in bold font.

Gene description	Down-reg FC	p-value	GenBank
Exportin-1	20.74	0.037	CB487200
Ubiquitin carboxyl-terminal hydrolase 5	6.35	0.016	CB496544
Protein FRA10AC1	6.33	0.025	EG835604
AF-4 proto-oncoprotein	6.20	0.016	CX027714
RNA-binding protein EWS	5.67	0.037	CB515604
Peroxiredoxin-5, mitochondrial precursor	4.83	0.004	CB493194
Glycylpeptide N-tetradecanoyltransferase 1	4.05	0.025	CB494396
FK506-binding protein 1A	4.04	0.010	CA049957
Ezrin	4.02	0.010	CA043385
Hemicentin-1 precursor	3.89	0.010	CB498739

involved in the regulation of cytotoxic stress-induced apoptosis (Saito et al., 2007) and Cdc37, a co-chaperone of Hsp90 involved in the promotion of cell growth (Hunter and Poon, 1997) were up-regulated (FC>3.5; Additional File 1).

Genes with the highest down-regulated fold change in the 2.4 g size class are displayed in Table 5b (FC>3). Transcripts involved in cell motility were down-regulated, such as adhesion-related integrin beta-7 precursor, involved in mucosal lymphocyte localization (Parker et al., 1992), and collagen alpha-3(VI) chain precursor, involved in connective tissue cell anchoring (FC>3, $p = 0.01$; Additional File 1). Metalloproteinase inhibitor 2 (*timp2*) was also down-regulated.

3.2. Microarray functional analysis

Gene lists were further analyzed through Gene Ontology (GO) and pathway analysis to interpret differential gene lists. Trimmed significantly enriched GO category lists ($p \leq 0.05$) are presented in Tables 6, 7 and 8, for the 0.3 g, 0.7 g and 2.4 g size groups, respectively. The full list of significantly enriched GO categories can be viewed in Additional File 2.

Functions indicated in the GO analysis of the 0.3 g group included cell structure, immune response, ion homeostasis, and negative regulation of cellular metabolism (Table 6). The category negative regulation of nucleobase, nucleoside, nucleotide and nucleic acid metabolic process was enriched (seven entities) and is a daughter group of the enriched category negative regulation of cellular metabolic process ($p = 0.01$; nine entities; Additional File 2). Enriched cell structure-related categories included cytoskeleton part and endoplasmic reticulum. Inflammation and ion transport categories were also enriched.

The 0.7 g differential gene list contained more enriched categories than the other two size groups, reflective of the larger input gene list. Functions in this list included catabolism, immune response, cell structure and motility, and iron handling (Table 7). Catabolic categories included digestion, hydrolase activity, and chitin catabolic process.

Table 4a
Up-regulated genes in the 0.7 g infected pink salmon with highest fold change (Mann–Whitney unpaired $p \leq 0.05$). Genes discussed in the text are in bold font.

Gene description	Up-reg FC	p-value	GenBank
Slime mold cyclic AMP receptor	13.39	0.016	CB507773
Radial spoke head 1 homolog	12.67	0.006	DY732411
Oxysterol-binding protein-related protein 6	9.89	0.037	CA063979
Forkhead box protein J3	9.64	0.010	DW583738
Sodium/glucose cotransporter 1	9.13	0.016	CA043404
Snurportin-1	8.34	0.006	EG758275
DNA topoisomerase 1	8.10	0.004	EG920165
Intraflagellar transport protein 46	7.99	0.037	CB518092
Mitochondrial ribosomal protein (VAR1)	7.58	0.010	CA037450
Talin-1	7.54	0.004	CA045263

Table 4b
Down-regulated genes in the 0.7 g infected pink salmon with highest fold change (Mann–Whitney unpaired $p \leq 0.05$). Genes discussed in the text are in bold font.

Gene description	Down-reg FC	p-value	GenBank
Titin	10.55	0.006	EG795798
26S proteasome non-ATPase regulatory subunit 12	9.12	0.037	CK990611
Copia protein	7.03	0.006	DY719895
Apolipoprotein A-I precursor	6.51	0.004	CB510585
Titin	6.11	0.004	EG868655
Syntaxin-18	6.10	0.010	DW539041
Nucleoside diphosphate kinase, mitochondrial precursor	5.99	0.037	CB510514
IT-I gene for isotocin	5.90	0.016	CA050111
Fatty acid-binding protein, adipocyte	5.81	0.037	CK990220
Intestinal mucin-like protein	5.79	0.004	CB510438

Immune response and lysozyme activity were also enriched. Cell structure and motility-related enriched categories included ruffle, cell projection, and actin cytoskeleton organization and biogenesis. Related to iron handling, ferroxidase activity was enriched; all 17 differentially expressed entities (16 down-regulated) in the category were ferritin subunits.

Functions in the 2.4 g enriched GO categories were related to cell motility and other cellular activities (Table 8). Cell motility-related categories included extracellular region part and cell projection. Other enriched categories included metal ion binding, enzyme activator activity, transferase activity, and receptor binding.

As was viewed among differential gene lists, GO categories were also distinct among the different size groups. Commonalities were identified between the categories enriched in the 0.7 g and 2.4 g groups, such as the enrichment of categories involved in cell structure and motility, including the category cell projection.

Pathway analysis was used to find functional patterns in a gene list by investigating for the enrichment of a pathway in a gene list. Only the differential gene list of the 2.4 g infected pink salmon ($FC \geq 2$; $p \leq 0.05$) contained significantly enriched pathways, and included cell adhesion molecules (CAMs), tryptophan metabolism, glycosphingolipid biosynthesis (lacto and neolacto series), and aminosugar metabolism. None of the other size classes tested produced significant pathways.

3.3. Real-time quantitative polymerase chain reaction

After quality control, a total of 21 GOIs were included in the analysis of all size classes. Calculated relative expression ratios of GOIs normalized by *actb* and *eif4h* are presented in Fig. 2. Most GOIs are separated into the functional categories of proliferation inhibition, ROS and immunity, and remodeling and motility.

Expression profiles of stress-related anti-proliferative genes further confirmed the general trends in the microarray data among

Table 5a
Up-regulated genes in the 2.4 g infected pink salmon with highest fold change (Mann–Whitney unpaired $p \leq 0.05$). Genes discussed in the text are in bold font.

Gene description	Up-reg FC	p-value	GenBank
Acidic mammalian chitinase precursor	8.58	0.025	CB511226
Retroviral integration site protein Fli-1 homolog	5.10	0.037	DW536407
ATP-binding cassette sub-family D member 3	5.02	0.016	CA056730
VAR1 Mitochondrial ribosomal protein	4.93	0.025	CK991139
Heterogeneous nuclear ribonucleoprotein L-like	4.11	0.004	DY693285
Pepsin A precursor	4.08	0.025	CB503148
Ligatin	4.00	0.016	DW556429
Protein phosphatase 1 L	3.97	0.016	DW554038
Ecto-ADP-ribosyltransferase 5 precursor	3.92	0.037	EG909433
Serine/threonine-protein phosphatase 2A 65 kDa regulatory subunit A beta isoform	3.73	0.037	CB506378

Table 5b
Down-regulated genes in the 2.4 g infected pink salmon with highest fold change (Mann–Whitney unpaired $p \leq 0.05$). Genes discussed in the text are in bold font.

Gene description	Down-reg FC	p-value	GenBank
Alpha-actinin-1	4.77	0.037	DW558198
Condensin-2 complex subunit D3	4.65	0.010	CA062925
Hemoglobin subunit alpha-4	3.97	0.016	CA770045
TGF-beta receptor type-1 precursor	3.76	0.037	CB499379
Histone H2AV	3.71	0.025	CB491527
Similar to Apolipoprotein C-I precursor	3.63	0.006	CA047039
Nuclear receptor interaction protein	3.60	0.025	CA050283
Ras-related GTP-binding protein A	3.41	0.016	CA057387
Chloride channel protein ClC-Kb	3.38	0.025	DW583374
Metalloproteinase inhibitor 2 precursor	3.27	0.010	CA059039

salmon size classes. These transcripts, including sestrin-1 (*sesn1*), transducer of erbB-2 1 (*tob1*), cyclin-dependent kinase 4 inhibitor B (*cdkn2b*), and B-cell translocation gene 1 protein (*btg1*) were only up-regulated in the 0.3 g pink salmon. Additionally, transcription factor DP-1 (*tfdp1*), involved in integrating cell cycle events with transcriptional apparatus (Bandara et al., 1993) was close to passing significance testing (FC = 1.6 down; $p = 0.064$). All of these transcripts remained unchanged due to infection in the 0.7 g size group. In the 2.4 g size group, those that were differentially regulated showed inverse expression profiles to the 0.3 g infected pink salmon (Fig. 2). Furthermore, in the 2.4 g size group, protein synthesis-related transcripts were up-regulated, including peptidyl-prolyl cis-trans isomerase (*fkbp7*), a member of a gene family involved in protein folding, and ribonuclease P protein subunit p21 (*rpp21*), which encodes a tRNA processor. Additionally, dual specificity protein phosphatase 26 (*dusp26*), involved in promoting cell proliferation by inhibiting apoptosis in human tumors (Yu et al., 2007), was also up-regulated in the 2.4 g group.

Tissue remodeling, previously implicated in the sensitivity of Atlantic salmon to *L. salmonis* (Skugor et al., 2008) requires cell motility, an identified function in our Gene Ontology analysis (Table 7). The qRT-PCR analysis confirmed involvement of the tissue remodeling function in the response to louse infection; matrix metalloproteinase family members *mmp9* and *mmp13* were up-regulated due to infection in the 0.3 g group by 2.5 folds and 2.9 folds ($p < 0.02$), respectively, and in the 0.7 g group by 3.3 folds ($p < 0.02$) and 6.4 folds ($p < 0.01$), respectively (Fig. 2). Tissue inhibitor of metalloproteinase-2 (*timp2*) did not show differential regulation in these size groups. However, consistent with microarray results, *timp2* was down-regulated in the 2.4 g group (FC = 1.5; $p < 0.01$), as was *mmp13* (FC = 3.4; $p < 0.02$). The similar expression of the matrix metalloproteinases in the 0.3 g and 0.7 g groups are one of the only strong similarities between the responses among these two size classes identified in this investigation.

Immune-relevant transcripts were differentially regulated only in the 2.4 g pink salmon (Fig. 2c). Nucleolysin (*tia1*), involved in cell-mediated killing, was up-regulated (FC = 1.3; $p < 0.01$). Gamma-interferon-inducible lysosomal thiol reductase (*ifi30*) was selected from microarray results as a possible Th2 response gene. This transcript showed a high level of individual variation in the qRT-PCR results (Fig. 2c), and did not pass significance testing, although it was close ($p = 0.056$). Superoxide dismutase-1 (*sod1*), a destroyer of toxic cellular radicals was selected to investigate the role of reactive oxygen species. This transcript remained unchanged in response to infection in all size groups.

Table 6
Trimmed Gene Ontology categories significantly enriched in the infected 0.3 g pink salmon bi-directional differentially expressed gene list. Includes the number of genes annotated with the GO term in the differential list compared to those annotated with the term on the array. Categories discussed in the text are in bold font.

GO category	Count in selection	Count in total	p-value	GO accession
Cytoskeletal part	14	295	0.001	0044430
Transcription factor binding	9	173	0.005	0008134
Inflammatory response	5	63	0.006	0006954
Multicellular organismal process	18	517	0.008	0032501
Ion transporter activity	7	154	0.025	0015075
Endoplasmic reticulum	7	158	0.029	0005783
Ion transport	5	94	0.031	0006811
Negative regulation of nucleobase, nucleoside, nucleotide and nucleic acid metabolic process	7	173	0.044	0045934

Table 7
Trimmed Gene Ontology categories significantly enriched in the infected 0.7 g pink salmon bi-directional differentially expressed gene list. Includes the number of genes annotated with the GO term in the differential list compared to those annotated with the term on the array. Categories discussed in the text are in bold font.

GO category	Count in selection	Count in total	p-value	GO accession
Response to acid	10	12	3.78E-09	0001101
Lysozyme activity	10	12	3.78E-09	0003796
Cell wall chitin metabolic process	10	12	3.78E-09	0006037
Response to fungus	10	12	3.78E-09	0009620
Chitinase activity	10	13	1.50E-08	0004568
Chitin catabolic process	10	13	1.50E-08	0006032
Chitin binding	10	13	1.50E-08	0008061
Ferroxidase activity	17	46	5.74E-07	0004322
Structural constituent of ribosome	28	118	5.42E-06	0003735
Sugar binding	14	39	8.53E-06	0005529
Structural molecule activity	53	299	8.66E-06	0005198
Digestion	11	26	1.29E-05	0007586
Carbohydrate binding	18	68	5.55E-05	0030246
Hydrolase activity, hydrolyzing O-glycosyl compounds	16	57	6.61E-05	0004553
Translation	26	121	7.28E-05	0006412
Macromolecule biosynthetic process	34	196	5.28E-04	0009059
Serine-type endopeptidase activity	18	86	0.0013	0004252
Nuclear matrix	9	30	0.0016	0016363
Hydrolase activity	111	887	0.0021	0016787
Actin cytoskeleton reorganization	5	12	0.0037	0031532
RNA binding	44	303	0.0039	0003723
Carbohydrate metabolic process	29	181	0.0045	0005975
Translational elongation	6	18	0.0054	0006414
Stress fiber	7	24	0.0062	0001725
Extracellular space	21	122	0.0063	0005615
Endopeptidase activity	31	203	0.0069	0004175
Phosphoinositide binding	6	19	0.0073	0035091
Translation elongation factor activity	5	14	0.0080	0003746
Cell projection	21	129	0.0119	0042995
Actin cytoskeleton organization and biogenesis	21	132	0.0153	0030036
COPI vesicle coat	6	22	0.0156	0030126
Ruffle	8	35	0.0165	0001726
Extracellular region part	34	243	0.0176	0044421
Heart morphogenesis	5	17	0.0193	0003007
Trypsin activity	6	24	0.0238	0004295
Muscle myosin complex	6	24	0.0238	0005859
Structural constituent of cytoskeleton	11	59	0.0244	0005200
Arp2/3 protein complex	5	18	0.0247	0005885
Embryonic development	11	60	0.0273	0009790
Amine metabolic process	17	110	0.0349	0009308
Multicellular organismal development	8	40	0.0351	0007275
Response to biotic stimulus	15	94	0.0357	0009607
Phosphoric monoester hydrolase activity	18	119	0.0369	0016791
Biopolymer catabolic process	17	112	0.0406	0043285
Myofibril assembly	6	27	0.0408	0030239
Immune response	20	138	0.0430	0006955
Cellular macromolecule catabolic process	18	122	0.0456	0044265

Table 8
Trimmed Gene Ontology categories significantly enriched in the infected 2.4 g pink salmon bi-directional differentially expressed gene list. Includes the number of genes annotated with the GO term in the differential list compared to those annotated with the term on the array. Categories discussed in the text are in bold font.

GO category	Count in selection	Count in total	p-value	GO accession
Extracellular region part	12	243	3.23E-04	0044421
Protein dimerization activity	7	152	0.0085	0046983
Transferase activity	22	861	0.0106	0016740
Metal ion binding	9	243	0.0118	0046872
Transferase activity, transferring hexosyl groups	5	91	0.0125	0016758
Enzyme activator activity	5	108	0.0244	0008047
Cation binding	7	188	0.0247	0043169
Receptor binding	7	192	0.0273	0005102
Extracellular space	5	122	0.0384	0005615
Cell projection	5	129	0.0469	0042995
Organelle organization and biogenesis	12	459	0.0470	0006996

4. Discussion

4.1. Transcriptome response overview and comparison

L. salmonis infections resulted in large transcriptome perturbations in all size classes of pink salmon investigated (Table 1). At 6 dpe, primary responses of the different size classes to the lice infection were profoundly different when compared to each other, as identified in differentially expressed gene lists (Fig. 1), enriched GO functional categories (Tables 6, 7, and 8), and qRT-PCR expression profiles (Fig. 2). This emphasizes the importance of considering each size class independently for louse sensitivity, including the 0.7 g and 2.4 g size classes, which did not show significant variation in mortality rates (Jones et al., 2008). Similarities among responses, although rare, also provide insight into the gradual development of resistance to the parasite as the salmon develops from sensitive (0.3 g) to competent (2.4 g). Limitations in the experimental design included the absence of the 2.4 g size class in the reference channel and multi-tissue sampling, which may have allowed for the capture of varying ratios of tissues among the different size groups. These limitations could confound cross-size class comparisons, however should not hinder within-size class comparisons. Additionally, one of the problems with both microarray and PCR analyses is the potential for cross-hybridization, or cross-reactivity, with other gene family members or duplicates, of particular relevance in the pseudotetraploid salmonids. For example, expression profiles of titin did not correspond completely to those identified in microarray results, which likely occurred due to alternate forms of the transcript cross-hybridizing to the microarray. Although many precautions were taken to eliminate this problem in qRT-PCR methods, such as the use of direct amplicon sequencing and qRT-PCR melt curve analysis, the complete genome is not yet known and we cannot fully eliminate the possible influence of this confounding factor.

Transcriptome profiling enabled the identification of potential detrimental effects in the 0.3 g infected pink salmon during the first week of infection that were therefore attributable to the attached copepodid stages of *L. salmonis*. This early time point of sampling was selected to investigate the primary responses to the infection, and should capture primary innate immune responses such as those identified early in the infection period in other Pacific salmon (Johnson and Albright, 1992). Additionally, the selection of this early time point allowed for the sampling of a broad range of responders, and thus prevented the confounding variable of only profiling the more robust surviving fish, which would have been more probable at later time points, particularly in the smallest size class.

Response trends in the sensitive 0.3 g pink salmon included inhibition of cell proliferation through the integration of cell stress signals accompanying inflammation and tissue remodeling. Main trends in the response of the competent 2.4 g pink salmon included growth and cell motility, with some immune response. The 0.7 g size class shared tissue remodeling with the 0.3 g pink salmon, although without inhibited cell proliferation, and shared cell motility with the 2.4 g pink salmon.

4.2. Sensitivity and growth

Juvenile 0.3 g pink salmon are sensitive to low-level, attached *L. salmonis* infections with indicators of stress-associated transcriptional profiles identifiable within a week of infection initiation (6 dpe). This stress is mainly identified by cell proliferation inhibition, and is followed later by mortality and decreased weight gain, which become evident between 13 and 37 dpe (Jones et al., 2008). The expression profiles of transcripts related to cell cycle progression and Gene Ontology enriched categories (Tables 4a, 4b and 6) indicate decreased proliferation, as presented in Sections 3.1 and 3.2. Profiles of up-regulated cell proliferation inhibition-related transcripts in the qRT-PCR analysis of the 0.3 g size class provide further evidence for this function (Fig. 2). These genes include up-regulation of *sesn1*, which can occur during in vitro cell starvation (Velasco-Miguel et al., 1999), and up-regulation of the in vitro cell proliferation suppressor *tob1*, which can indicate unresponsive T-cells (Maekawa et al., 2002; Tzachanis et al., 2001). Additionally, up-regulation of *btg1*, a member of the same anti-proliferative family as *tob1*, has been shown to be up-regulated at G_0/G_1 halting and down-regulated as the cells move through G_1 (Rouault et al., 1992). CDKN2b binds and inhibits Cdk2, an important G_1/S transition protein, and the up-regulation of its transcript can indicate cell cycle arrest induced by interferon-α (Sangfelt et al., 1999) or by TGF-β in keratinocytes (Reynisdóttir et al., 1995). Differential expression of such a diverse range of transcripts towards a function of anti-proliferation may be indicating that cell cycle events are being integrated with the transcriptional machinery in the juvenile infected pink salmon. Integration for cell cycle proliferation induction can be conducted by transcription factors (TF), such as DRTF1/E2F, which can be activated by synergistic interactions of TFDP1 and E2F-1 (Bandara et al., 1993). We investigated the expression of *tfdp1*, as a reduction of this signal could potentially occur through reduction of these interacting factors, but the expression was not significantly different from control (Fig. 2a; FC>1.5; $p=0.064$). Transcription changes in the 0.3 g juvenile pink salmon indicate cell stress, which is not evident in the larger size groups tested.

Cell stress and decreased proliferation in the 0.3 g juvenile pink salmon may be derived from parasite-induced nutrient diversion, and therefore the sensitivity in this size group could be related to a lack of nutrients during a life stage of rapid growth (Heard, 1991). From the results presented here, it is not possible to detect if nutrients are being directly lost to the parasite or are being indirectly lost due to host responses to the parasite. Both are possible, as parasitism can directly reduce growth (Fernandez and Esch, 1991), as can host responses to parasitism, such as long term cortisol exposure and chronic inflammation (Barton et al., 1987; DeBenedetti et al., 1997). Nutrient limitation or inappropriate nutrient partitioning at a key growth stage may be contributing to the sensitivity of this size group.

Inappropriate nutrient partitioning may occur via increased inflammation or tissue remodeling. These processes are indicated in the 0.3 g size group by enriched Gene Ontology categories, and by the up-regulation of *mmp9* and *mmp13* (Fig. 2). In the susceptible Atlantic salmon, *L. salmonis* infections may become chronic due to increased inflammation and matrix metalloproteinase-dependent tissue remodeling without accompanying cell proliferation (Skugor et al., 2008). *Mmp9* has been shown to have a role in both the initiation and resolution of inflammation in teleosts (Chadzinska et al., 2008). Increased expression of *mmp9* and *mmp13* in the 0.3 g infected pink

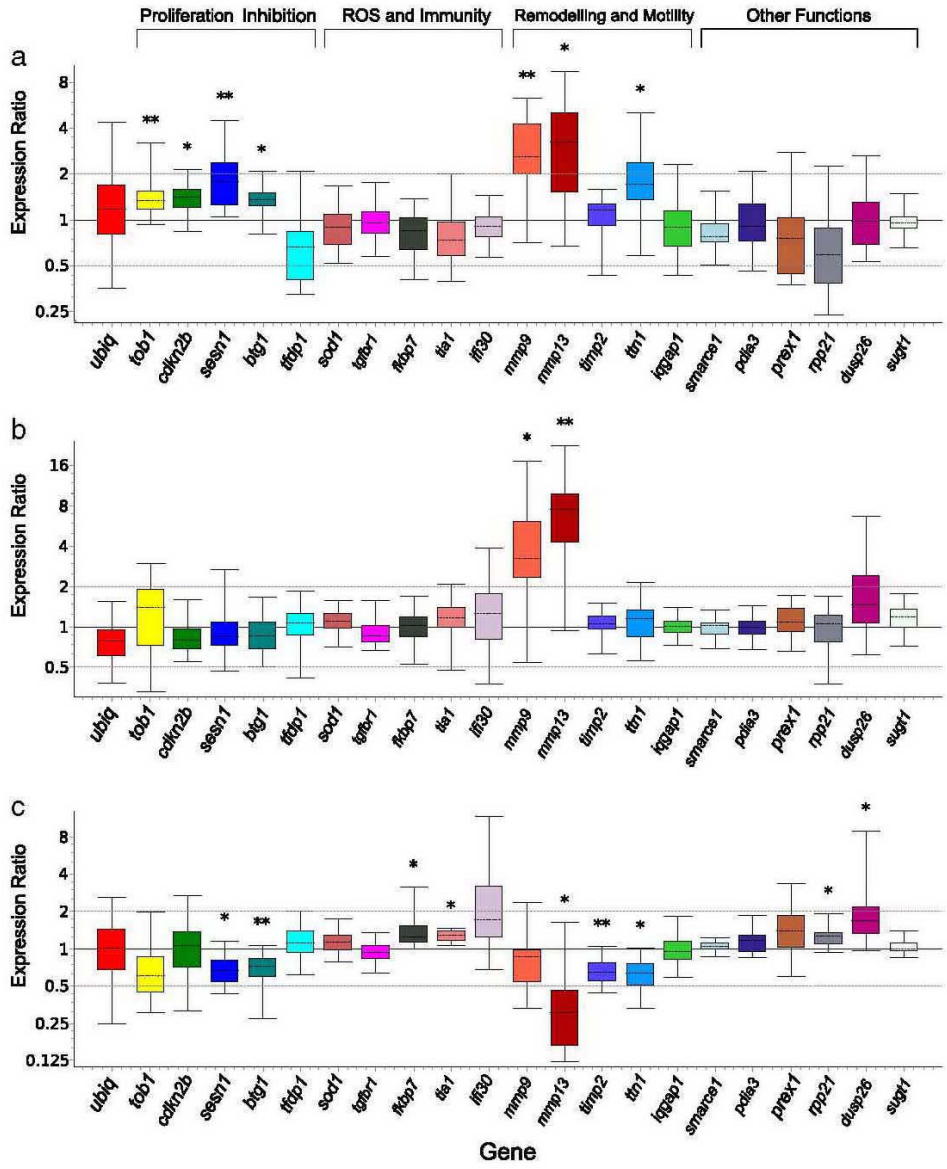

Fig. 2. qRT-PCR gene profiles in statistical whisker-box plots of expression ratios of genes of interest in response to infection in the (a) 0.3 g, (b) 0.7 g, and (c) 2.4 g size groups. Expression ratios are relative to control samples and are normalized by the geometric mean of expression levels of *eif4h* and *actb*. Ubiquitin is included on the graph as an example of a potential normalizer gene, that did not end up being used to normalize. Box area, whiskers and hatched line in box display interquartile range, upper or lower quartiles, and median, respectively. Y-axis scales are different for the different size groups (a–c), and each size group should be considered individually. Significance was determined by Pair Wise Fixed Reallocation Randomization Test©, *denotes $p \leq 0.05$ **denotes $p \leq 0.01$.

salmon accompanies the aforementioned cell proliferation inhibition (Fig. 2a). Furthermore, although these two transcripts were up-regulated to a greater extent in the 0.7 g infected pink salmon, the accompanying cell proliferation inhibition was absent (Fig. 2b), as was the mortality and weight gain (Jones et al., 2008). Inflammation with inhibited cell proliferation appears to be a distinguishing feature of the incompetent response to *L. salmonis* in the susceptible 0.3 g size class of pink salmon.

Metabolism and growth in the 0.7 g and 2.4 g size classes do not mirror the responses of the younger 0.3 g size group in response to the *L. salmonis* infection. The infected 0.7 g pink salmon display changes to nutrient processing transcripts, with enriched Gene Ontology categories digestion and hydrolase activity (Table 7), and stable expression of qRT-PCR-investigated cell proliferation-related transcripts (Fig. 2b). The differential transcriptome of the 2.4 g infected pink salmon included genes involved in protein stabilization and cell proliferation. For example, up-regulation of protein phosphatase 1L and Cdc37, and down-regulation of *timp2* were identified with high fold change (Tables 5a and 5b). Up-regulation of Cdc37, a co-chaperone of Hsp90, is important for cell growth (Hunter and Poon, 1997). *Timp2* up-regulation can block EGF-mediated mitogenic signaling (Hoegy et al., 2001), and it is therefore interesting to note the down-regulation in the 2.4 g salmon (Fig. 2c). Additionally, the 2.4 g infected salmon showed up-regulation of protein folding family member *fkbp7*, cell proliferation promoter *dusp26*, and tRNA processor *rpp21* (Fig. 2c). Cell proliferation inhibition transcripts identified

from the 0.3 g infected salmon were either static, or down-regulated in the 2.4 g infected salmon, including down-regulation of both *sesn1* and *btg1* (Fig. 2c). *Sesn1* down-regulation can occur when androgen receptors are activated by the ligands testosterone or dihydrotestosterone (Wang et al., 2006), and progression into G_1 phase requires down-regulation of *btg1* (Rouault et al., 1992).

In addition to the differential expression of the aforementioned growth-related transcripts, one population of infected 2.4 g pink salmon was found to have a slight, but significant increase in weight gain at the end of the 37 day infection trial (Jones et al., 2008). More work would need to be done to confirm this apparent increased growth. All pink salmon from this exposure were planktivorous, and would feed on copepods in their natural environment (Heard, 1991). The 2.4 g size class may have gained nutrients by feeding on lice introduced to the tank during the exposure, although the salmon were sedated at the time of the exposure and no filter was in place to keep lice in the tank after flow rates were resumed. The activity of the aforementioned growth-related transcripts in the 2.4 g salmon six days after the exposure indicates that this growth increase is continuing throughout the exposure, after all unattached copepodids were presumably removed from the tank by flow rates. Grazing of mobile *L. salmonis* by cleaner fish, such as threespine stickleback (*Gasterosteus aculeatus*) has been documented (Losos et al., 2010), but we are not aware of any cases of salmon grazing *L. salmonis* off of each other. Additionally, the lice present at 6 dpe are attached copepodids, thus much smaller than those in the aforementioned stickleback study.

Alternately, the infection with *L. salmonis* after a size threshold may be inducing a parasite-induced growth in the larger juvenile pink salmon. Low-level parasite infections have been shown to increase growth rates of immature hosts (reviewed in Phares, 1996), including threespine stickleback infected experimentally with a cestode parasite (Arnott et al., 2000), and naturally-infected developing whitefish (*Coregonus laveratus*; Pulkkinen and Valtonen, 1999). In host-castrating systems, increased host growth only occurs in instances of infection prior to reproductive maturity (Keas and Esch, 1997). In non-castrating systems, low-level infections and sympatric host-parasite systems result in the fastest parasite-induced host growth (Ballabeni, 1994). Interestingly, the 2.4 g pink salmon in this study meet all of the above criteria necessary for parasite-induced growth. Furthermore, in other host-parasite systems, changes to host growth can occur through parasite-derived secreted growth hormone receptor agonists (Phares, 1996). As some bioactive substances have already been identified and characterized in *L. salmonis* secretions (Fast et al., 2007), this could be an avenue of further research if other work supports this association between infection and increased growth. It would also be useful to investigate relative host reproductive success in the previously-infected and control individuals upon reaching reproductive maturity, as parasite-induced growth can occur at a cost to reproductive fitness (Baudoin, 1975). Additionally, in louse exposure experiments utilizing lethal sampling, gut content analysis would be helpful to understand the extent of the differential feeding of these fish on the infecting ectoparasite.

Increased growth is not observed in the 0.7 g infected pink salmon. The response of the 0.7 g size class is less apparent, but appears to be a transitional stage between the reduced growth (0.3 g) and the increased growth (2.4 g) stages. The transcriptomic responses of the 0.7 g and 2.4 g pink salmon do not indicate systemic stress, as is suggested from the 0.3 g infected pink salmon.

4.3. Immunological responses

Salmon immune-modulation has been documented in vitro resulting from *L. salmonis* secretions (Fast et al., 2007). The identified up-regulation of matrix metalloproteinase expression in the 0.3 g and 0.7 g pink salmon may be due to immune modulation caused by parasite secretions. Prostaglandin E_2 (PGE_2), a component of louse secretions (Fast et al., 2004) induces increased *mmp9* expression in mice (Yen et al., 2008). Louse secretions are elicited by host skin mucus and are variable depending on host species (Fast et al., 2003). If the release of PGE_2 is equal among members of the same host species, smaller fish are potentially subjected to higher plasma concentrations and increased downstream effects. However, to conclusively say if this was a factor, more work would need to be done.

The identification of ferritin up-regulation in the 0.7 g infected pink salmon may be indicative of iron sequestering to prevent parasitic acquisition. Previous work has shown an increase in transferrin in adult Atlantic salmon in response to the louse infection, and it was hypothesized as a method of reducing iron availability to the parasite (Easy and Ross, 2009).

Cellular motility and immune response appear to be affected by the infection in the 0.7 g and 2.4 g pink salmon, possibly indicating immune cell migration, wound healing or both. Although similarities between host responses of the different size classes are rare, differentially expressed cell motility transcripts were identified in both the 0.7 g and 2.4 g groups, as presented in Section 3.1. Additionally, as mentioned in Section 3.2, Gene Ontology categories involving cell motility were enriched in both the 0.7 g and the 2.4 g infected salmon (Table 7 and 8), and one of the pathways enriched in the 2.4 g transcriptome profile was cell adhesion molecules (CAMs), involved in anchoring migrating cells to a target.

Although cell motility activity was present in the transcriptome response, few direct effectors of immune response were identified. Of the immune-related genes investigated with qRT-PCR, most had high variation among individuals, including IFN-γ-induced lysosomal thioreductase (*ifi30*) and did not pass significance testing (Fig. 2c; $FC>2$; $p=0.056$). IFI30 denatures proteins by reducing disulfide bonds, and may have a role in antigen processing in antigen presenting cells (Arunachalam et al., 2000). Significantly up-regulated in the 2.4 g infected salmon was nucleolysin (*tia1*), an indicator of neutrophil nucleolytic activity and of the induction of apoptosis in cytotoxic T lymphocyte target cells (Tian et al., 1991). Neutrophils have a role in the defense responses of coho salmon to sea lice (Johnson and Albright, 1992).

5. Conclusions

Pink salmon size classes responded differently to *L. salmonis* infections, and susceptibility markers in the 0.3 g salmon appeared early in the response to the smaller and less damaging attached stages of lice. Susceptibility may be related to nutrient diversion at a rapidly growing life stage, and energy may be diverted to accommodate incompetent immune responses and tissue remodeling. Although 0.5 g pink salmon develop a protective response after vaccination with bacterial antigens (Johnson et al., 1982), immune responses of the 0.3 g infected fish did not parallel those measured in the larger size groups; inflammation and tissue remodeling may be exacerbating the effects of infection. Host immune modulation by bioactive agents present in sea louse saliva may also play a role in the susceptibility, as the smaller fish may experience higher concentrations due to size ratios. Important roles of cell motility and nucleolytic activity were evident in the responses of the larger size classes of pink salmon. Additionally, *L. salmonis* infection may result in an increased growth rate of the juvenile pink salmon after they pass a certain size threshold, as was observed in the 2.4 g pink salmon. We have generated and analyzed large transcriptome datasets reflective of juvenile pink salmon responses to *L. salmonis* infections, and in doing so, have increased our understanding of the complexity of this ecologically-relevant host–parasite system.

Acknowledgments

This research was funded by Genome British Columbia, the Province of British Columbia, the University of Victoria, Greig Seafood, Mainstream

Canada, Microtek International, and Marine Harvest. Thanks to E Kim and G Prosperi-Porta for maintaining, harvesting and processing fish samples. Thanks to T Lundrigan for assistance in aRNA synthesis and to E Rondeau for amplicon sequencing. Thanks to G Cooper for assistance in microarray techniques and experimental design. Thanks to N Veldhoen, S Pavey, and A Bridle for discussions on qRT-PCR experimental design. Thanks to K von Schalburg for assistance with primer design and for constructive criticism on this manuscript. Thanks to the members of the Koop lab for the support.

Appendix A. Supplementary data

Supplementary data to this article can be found online at doi:10.1016/j.cbd.2011.04.001.

References

Arnott, S.A., Barber, I., Huntingford, F.A., 2000. Parasite-associated growth enhancement in a fish-cestode system. Proc. Biol. Sci. 267, 657–663.

Arunachalam, B., Phan, U.T., Geuze, H.J., Cresswell, P., 2000. Enzymatic reduction of disulfide bonds in lysosomes: characterization of a gamma-interferon-inducible lysosomal thiol reductase (GILT). Proc. Natl. Acad. Sci. U.S.A. 97, 745–750.

Ballabeni, P., 1994. Experimental differences in mortality patterns between European minnows, *Phoxinus phoxinus*, infected with sympatric or allopatric trematodes, *Diplostomum phoxini*. J. Fish Biol. 45, 257–267.

Bandara, L.R., Buck, V.M., Zamanian, M., Johnston, L.H., La Thangue, N.B., 1993. Functional synergy between DP-1 and E2F-1 in the cell cycle-regulating transcription factor DRTF1/E2F. EMBO J. 12, 4317–4324.

Barton, B.A., Schreck, C.B., Barton, L.D., 1987. Effects of chronic cortisol administration and daily acute stress on growth, physiological conditions, and stress responses in juvenile rainbow trout. Dis. Aquat. Org. 2, 173–185.

Baudoin, M., 1975. Host castration as a parasitic strategy. Evolution 29, 335–352.

Bowers, J.M., Mustafa, A., Speare, D.J., Conboy, G.A., Brimacombe, M., Sims, D.E., Burka, J.F., 2000. The physiological response of Atlantic salmon, *Salmo salar* L., to a single experimental challenge with sea lice, *Lepeophtheirus salmonis*. J. Fish Dis. 23, 165–172.

Bron, J.E., Sommerville, C., Rae, G.H., 1993. The functional morphology of the alimentary canal of larval stages of the parasitic copepod *Lepeophtheirus salmonis*. J. Zool. 230, 207–220.

Burridge, K., Fath, K., Kelly, T., Nuckolls, G., Turner, C., 1988. Focal adhesions: transmembrane junctions between the extracellular matrix and the cytoskeleton. Annu. Rev. Cell Dev. Biol. 4, 487–525.

Chadzinska, M., Baginski, P., Kolaczkowska, E., Savelkoul, H.F.J., Verburg-van Kemenade, B.M.L., 2008. Expression profiles of matrix metalloproteinase 9 in teleost fish provide evidence for its active role in initiation and resolution of inflammation. Immunology 125, 601–610.

Costello, M.J., 2006. Ecology of sea lice parasitic on farmed and wild fish. Trends Parasitol. 22, 475–483.

DeBenedetti, F., Alonzi, T., Moretta, A., Lazzaro, D., Costa, P., Poli, V., Martini, A., Ciliberto, G., Fattori, E., 1997. Interleukin 6 causes growth impairment in transgenic mice through a decrease in insulin-like growth factor-I — a model for stunted growth in children with chronic inflammation. J. Clin. Invest. 99, 643–650.

Easy, R.H., Ross, N.W., 2009. Changes in Atlantic salmon (*Salmo salar*) epidermal mucus protein composition profiles following infection with sea lice (*Lepeophtheirus salmonis*). Comp. Biochem. Physiol. Part D Genomics Proteomics 4, 159–167.

Fast, M.D., Ross, N.W., Mustafa, A., Sims, D.E., Johnson, S.C., Conboy, G.A., Speare, D.J., Johnson, G., Burka, J.F., 2002. Susceptibility of rainbow trout *Oncorhynchus mykiss*, Atlantic salmon *Salmo salar* and coho salmon *Oncorhynchus kisutch* to experimental infection with sea lice *Lepeophtheirus salmonis*. Dis. Aquat. Org. 52, 57–68.

Fast, M.D., Burka, J.F., Johnson, S.C., Ross, N.W., 2003. Enzymes released from *Lepeophtheirus salmonis* in response to mucus from different salmonids. J. Parasitol. 89, 7–13.

Fast, M.D., Ross, N.W., Craft, C.A., Locke, S.J., MacKinnon, S.L., Johnson, S.C., 2004. *Lepeophtheirus salmonis*: characterization of prostaglandin E-2 in secretory products of the salmon louse by RP-HPLC and mass spectrometry. Exp. Parasitol. 107, 5–13.

Fast, M.D., Ross, N.W., Johnson, S.C., 2005. Prostaglandin E-2 modulation of gene expression in an Atlantic salmon (*Salmo salar*) macrophage-like cell line (SHK-1). Dev. Comp. Immunol. 29, 951–963.

Fast, M.D., Johnson, S.C., Eddy, T.D., Pinto, D., Ross, N.W., 2007. *Lepeophtheirus salmonis* secretory/excretory products and their effects on Atlantic salmon immune gene regulation. Parasite Immunol. 29, 179–189.

Fernandez, J., Esch, G.W., 1991. Effect of parasitism on the growth rate of the pulmonate snail *Helisoma anceps*. J. Parasitol. 77, 937–944.

Finstad, B., Bjørn, P.A., Grimnes, A., Hvidsten, N.A., 2000. Laboratory and field investigations of salmon lice *Lepeophtheirus salmonis* (Krøyer) infestation on Atlantic salmon (*Salmo salar* L.) post-smolts. Aquacult. Res. 31, 795–803.

Firth, K.J., Johnson, S.C., Ross, N.W., 2000. Characterization of proteases in the skin mucus of Atlantic salmon (*Salmo salar*) infected with the salmon louse (*Lepeophtheirus salmonis*) and in whole-body louse homogenate. J. Parasitol. 86, 1199–1205.

Grimnes, A., Jakobsen, P.J., 1996. The physiological effects of salmon lice infection on post-smolt of Atlantic salmon. J. Fish Biol. 48, 1179–1194.

Heard, W.R., 1991. Life history of pink salmon (*Oncorhynchus gorbuscha*), In: Groot, C., Margolis, L. (Eds.), Pacific Salmon Life Histories, 1st ed. UBC Press, Vancouver, pp. 177–181.

Hoegy, S.E., Oh, H.R., Corcoran, M.L., Stetler-Stevenson, W.G., 2001. Tissue inhibitor of metalloproteinases-2 (TIMP-2) suppresses TKR-growth factor signaling independent of metalloproteinase inhibition. J. Biol. Chem. 276, 3203–3214.

Hou, Y.Q., Qin, H.M., Follit, J.A., Pazour, G.J., Rosenbaum, J.L., Witman, G.B., 2007. Functional analysis of an individual IFT protein: IFT46 is required for transport of outer dynein arms into flagella. J. Cell Biol. 176, 653–665.

Hunter, T., Poon, R.Y.C., 1997. Cdc37: a protein kinase chaperone? Trends Cell Biol. 7, 251-251.

Hynes, R.O., 1992. Integrins: versatility, modulation, and signaling in cell adhesion. Cell 69, 11–25.

Johnson, S.C., Albright, L.J., 1991. The developmental stages of *Lepeophtheirus salmonis* (Krøyer, 1837) (Copepoda: Caligidae). Can. J. Zool. 69, 929–950.

Johnson, S.C., Albright, L.J., 1992. Comparative susceptibility and histopathology of the response of naive Atlantic, chinook and coho salmon to experimental infection with *Lepeophtheirus salmonis* (Copepoda: Caligidae). Dis. Aquat. Org. 14, 179–193.

Johnson, K.A., Flynn, J.K., Amend, D.F., 1982. Onset of immunity in salmonid fry vaccinated by direct immersion in *Vibrio anguillarum* and *Yersinia ruckeri* bacterins. J. Fish Dis. 5, 197–205.

Jones, S.R.M., 2009. Controlling salmon lice on farmed salmon and implications for wild salmon. CAB Rev. 4, 1–13.

Jones, S.R.M., Fast, M.D., Johnson, S.C., Groman, D.B., 2007. Differential rejection of salmon lice by pink and chum salmon: disease consequences and expression of proinflammatory genes. Dis. Aquat. Org. 75, 229–238.

Jones, S., Kim, E., Bennett, W., 2008. Early development of resistance to the salmon louse, *Lepeophtheirus salmonis* (Krøyer), in juvenile pink salmon, *Oncorhynchus gorbuscha* (Walbaum). J. Fish Dis. 31, 591–600.

Keas, B.E., Esch, G.W., 1997. The effect of diet and reproductive maturity on the growth and reproduction of *Helisoma anceps* (Pulmonata) infected by *Halipegus occidualis* (Trematoda). J. Parasitol. 83, 96–104.

Koop, B.F., von Schalburg, K.R., Leong, J., Walker, N., Lieph, R., Cooper, G.A., Robb, A., Beetz-Sargent, M., Holt, R.A., Moore, R., Brahmbhatt, S., Rosner, J., Rexroad, C.E., McGowan, C.R., Davidson, W.S., 2008. A salmonid EST genomic study: genes, duplications, phylogeny and microarrays. BMC Genomics 9.

Kudo, N., Khochbin, S., Nishi, K., Kitano, K., Yanagida, M., Yoshida, M., Horinouchi, S., 1997. Molecular cloning and cell cycle-dependent expression of mammalian CRM1, a protein involved in nuclear export of proteins. J. Biol. Chem. 272, 29742–29751.

Labeit, S., Kolmerer, B., 1995. Titins: giant proteins in charge of muscle ultrastructure and elasticity. Science 270, 293–296.

Li, C.F., MacDonald, J.R., Wei, R.Y., Ray, J., Lau, K., Kandel, C., Koffman, R., Bell, S., Scherer, S.W., Alman, B.A., 2007. Human sterile alpha motif domain 9, a novel gene identified as down-regulated in aggressive fibromatosis, is absent in the mouse. BMC Genomics 8.

Losos, C.J.C., Reynolds, J.D., Dill, L.M., 2010. Sex-selective predation by threespine sticklebacks on sea lice: a novel cleaning behaviour. Ethology 116, 981–989.

Mackinnon, B.M., 1993. Host response of Atlantic salmon (*Salmo salar*) to infection by sea lice (*Caligus elongatus*). Can. J. Fish. Aquat. Sci. 50, 789–792.

Maekawa, M., Nishida, E., Tanoue, T., 2002. Identification of the anti-proliferative protein Tob as a MAPK substrate. J. Biol. Chem. 277, 37783–37787.

Nagasawa, K., Ishida, Y., Ogura, M., Tadokoro, K., Hiramatsu, K., 1993. The abundance and distribution of *Lepeophtheirus salmonis* (Copepoda: Caligidae) on six species of Pacific salmon in offshore waters of the North Pacific Ocean and Bering Sea, In: Boxshall, G., Defaye, D. (Eds.), Pathogens of Wild and Farmed Fish: sea lice, 1st ed. CRC Press, pp. 166–178.

Parker, C.M., Cepek, K.L., Russell, G.J., Shaw, S.K., Posnett, D.N., Schwarting, R., Brenner, M.B., 1992. A family of beta-7 integrins on human mucosal lymphocytes. Proc. Natl. Acad. Sci. U.S.A. 89, 1924–1928.

Pérez, R., Tupac-Yupanqui, I., Dunner, S., 2008. Evaluation of suitable reference genes for gene expression studies in bovine muscular tissue. BMC Mol. Biol. 9.

Pfaffl, M.W., Horgan, G.W., Dempfle, L., 2002. Relative expression software tool (REST©) for group-wise comparison and statistical analysis of relative expression results in real-time PCR. Nucleic Acids Res. 30.

Phares, K., 1996. An unusual host-parasite relationship: the growth hormone-like factor from plerocercoids of spirometrid tapeworms. Int. J. Parasitol. 26, 575–588.

Pulkkinen, K., Valtonen, E.T., 1999. Accumulation of plerocercoids of *Triaenophorus crassus* in the second intermediate host *Coregonus lavaretus* and their effect on growth of the host. J. Fish Biol. 55, 115–126.

Reynisdóttir, I., Polyak, K., Iavarone, A., Massagué, J., 1995. Kip/Cip and Ink4 Cdk inhibitors cooperate to induce cell cycle arrest in response to TGF-beta. Genes Dev. 9, 1831–1845.

Rouault, J.P., Rimokh, R., Tessa, C., Paranhos, G., Ffrench, M., Duret, L., Garoccio, M., Germain, D., Samarut, J., Magaud, J.P., 1992. *BTG1*, a member of a new family of antiproliferative genes. EMBO J. 11, 1663–1670.

Rozen, S., Skaletsky, H., 2000. Primer3 on the WWW for general users and for biologist programmers. Methods Mol. Biol. 132, 365–386.

Saito, J., Toriumi, S., Awano, K., Ichijo, H., Sasaki, K., Kobayashi, T., Tamura, S., 2007. Regulation of apoptosis signal-regulating kinase 1 by protein phosphatase 2C epsilon. Biochem. J. 405, 591–596.

Sangfelt, O., Erickson, S., Castro, J., Heiden, T., Gustafsson, A., Einhorn, S., Grandér, D., 1999. Molecular mechanisms underlying interferon-alpha-induced G0/G1 arrest: CKI-mediated regulation of G1 Cdk-complexes and activation of pocket proteins. Oncogene 18, 2798–2810.

Skugor, S., Glover, K.A., Nilsen, F., Krasonov, A., 2008. Local and systemic gene expression responses of Atlantic salmon (*Salmo salar* L.) to infection with the salmon louse (*Lepeophtheirus salmonis*). BMC Genomics 9, 1–18.

Tian, Q.S., Streuli, M., Saito, H., Schlossman, S.F., Anderson, P., 1991. A polyadenylate binding protein localized to the granules of cytolytic lymphocytes induces DNA fragmentation in target cells. Cell 67, 629–639.

Tzachanis, D., Freeman, G.J., Hirano, N., van Puijenbroek, A., Delfs, M.W., Berezovskaya, A., Nadler, L.M., Boussiotis, V.A., 2001. Tob is a negative regulator of activation that is expressed in anergic and quiescent T cells. Nat. Immunol. 2, 1174–1182.

Vandesompele, J., De Preter, K., Pattyn, F., Poppe, B., Van Roy, N., De Paepe, A., Speleman, F., 2002. Accurate normalization of real-time quantitative RT-PCR data by geometric averaging of multiple internal control genes. Genome Biol. 3.

Velasco-Miguel, S., Buckbinder, L., Jean, P., Gelbert, L., Talbott, R., Laidlaw, J., Seizinger, B., Kley, N., 1999. PA26, a novel target of the p53 tumor suppressor and member of the GADD family of DNA damage and growth arrest inducible genes. Oncogene 18, 127–137.

Vogel, B.E., Hedgecock, E.M., 2001. Hemicentin, a conserved extracellular member of the immunoglobulin superfamily, organizes epithelial and other cell attachments into oriented line-shaped junctions. Development 128, 883–894.

von Schalburg, K.R., Rise, M.L., Cooper, G.A., Brown, G.D., Gibbs, A.R., Nelson, C.C., Davidson, W.S., Koop, B.F., 2005. Fish and chips: various methodologies demonstrate utility of a 16,006-gene salmonid microarray. BMC Genomics 6.

Wagner, G.N., McKinley, R.S., Bjørn, P.A., Finstad, B., 2003. Physiological impact of sea lice on swimming performance of Atlantic salmon. J. Fish Biol. 62, 1000–1009.

Wagner, G.N., Fast, M.D., Johnson, S.C., 2008. Physiology and immunology of *Lepeophtheirus salmonis* infections of salmonids. Trends Parasitol. 24, 176–183.

Wang, G., Jones, S.J.M., Marra, M.A., Sadar, M.D., 2006. Identification of genes targeted by the androgen and PKA signaling pathways in prostate cancer cells. Oncogene 25, 7311–7323.

Wright, E.M., Turk, E., 2004. The sodium/glucose cotransport family SLC5. Pflugers Arch. 447, 510–518.

Yen, J.H., Khayrullina, T., Ganea, D., 2008. PGE2-induced metalloproteinase-9 is essential for dendritic cell migration. Blood 111, 260–270.

Yu, W., Imoto, I., Inoue, J., Onda, M., Emi, M., Inazawa, J., 2007. A novel amplification target, DUSP26, promotes anaplastic thyroid cancer cell growth by inhibiting p38 MAPK activity. Oncogene 26, 1178–1187.